

Postischemic administration of liposome-encapsulated luteolin prevents against ischemia-reperfusion injury in a rat middle cerebral artery occlusion model

Gang Zhao^{a,b}, Shao-Yun Zang^{a,b}, Zhi-Hua Jiang^{a,b}, Yao-Yue Chen^{a,b}, Xun-He Ji^{a,b}, Bu-Feng Lu^{a,b}, Jia-Hu Wu^a, Guo-Wei Qin^c, Li-He Guo^{a,b,*}

^aCell Star Bio-Technologies Co., Limited, Shanghai 201203, People's Republic of China

^bInstitute of Biochemistry and Cell Biology, Shanghai Institutes for Biological Sciences, Chinese Academy of Sciences, Shanghai 200031, People's Republic of China

^cInstitute of Materia Medica, Shanghai Institutes for Biological Sciences, Chinese Academy of Sciences, Shanghai 201203, People's Republic of China

Received 10 February 2010; received in revised form 24 April 2010; accepted 28 July 2010

Abstract

Oxidative stress-induced neuronal cell death has been implicated in neurodegenerative diseases; one such disease is ischemic stroke. Using reactive oxygen species (ROS)-insulted primary neurons, we screened neuroprotectants with clinical potential and then, using ischemia/reperfusion (I/R) model, investigated the anti-ischemic potential of candidate neuroprotectants. Here, we showed that luteolin, isolated from the ripe fruit of *Perilla frutescens* (L.) Britt, exhibited a neuroprotective action upon the in vitro platform, thus serving as candidate for in vivo pharmacological evaluation. Liposome-encapsulated luteolin produced dramatic preventing effects on I/R-induced behavioral and histological injuries after a 13-day post-ischemic treatment. Furthermore, this phytochemical not only lowered the increased level of mitochondrial ROS but also substantially up-regulated the decreased activity of catalase and glutathione in I/R rat brains. Collectively, luteolin as a neuroprotectant acts by anti-ischemic activity likely through a rebalancing of pro-oxidant/antioxidant status. Its multitarget mechanisms implicate potential effectiveness for clinically treating ischemia stroke.

© 2011 Elsevier Inc. All rights reserved.

Keywords: Reactive oxygen species; Luteolin; Neuroprotectant; Ischemia; Reperfusion; Oxidant-antioxidant balance

1. Introduction

Ischemic stroke is the third leading cause of death worldwide after heart disease and cancer and the single largest cause of long-lasting disability in developed countries [1,2]. Cerebral ischemia results from a transient or permanent reduction in cerebral blood flow that is restricted to the territory of a major brain artery. During its development, ischemia/reperfusion (I/R) injury is proven a major pathophysiological process including a series of phenomena such as excitotoxicity, oxidative stress, inflammation and apoptosis [3,4], each of which is entwined with mitochondrial dysfunction, releases of glutamate and proinflammatory mediators, decrease of ATP, reactive oxygen species (ROS) production and/or lipid peroxidation. Nonetheless, much attention has recently been drawn to the role of oxidative free radicals in the pathogenesis of ischemic stroke.

Rapid oxidative metabolic activity, high polyunsaturated fatty acid content, relatively low antioxidant capacity, and inadequate neuronal

repair activity [5,6] are underlying factors that define the susceptibility of cerebral tissue to ROS insult. ROS, including superoxide anion ($O_2^{\cdot-}$), hydrogen peroxide (H_2O_2), and the hydroxyl radical (OH^{\cdot}) [7], are commonly regarded as the earliest and most important pathogens for brain injury in the process of reducing blood supply and subsequently reperusing the ischemic cerebral regions [8]. Such brain damage by ROS insult has been considered to be involved in neuronal apoptosis [9,10], which has previously been suggested to initiate at molecular levels in ischemic or post-ischemic reperused regions especially penumbra [11]. Besides, the notion of ROS's contribution to neuronal apoptosis and degeneration is supported by the fact that a series of antioxidant compounds have propensities to delay neuronal apoptosis and protect against neurodegenerative procession [12].

A growing body of evidence demonstrates that varieties of herb materials exert an antioxidant activity; one such herb material is *Perilla frutescens* (L.) Britt. [13,14], from which we have isolated a polyphenolic constituent luteolin [15]. Luteolin, as a plant-derived compound with properties of anti-inflammatory, antiallergenic, antiviral and anticarcinogenic actions [16], is effective for attenuation of multiple sclerosis [17] and rheumatoid arthritis [18,19]. Besides, it has been proven to ameliorate anxiety [20] and amnesia [21] and been proposed as an inhibitor of β -site amyloid precursor protein-cleaving enzyme-1 [22]. This compound is also proven a potent

* Corresponding author. Institute of Biochemistry and Cell Biology, Shanghai Institutes of Biological Sciences, Chinese Academy of Sciences, Shanghai 200031, People's Republic of China. Tel.: +86 21 54921392; fax: +86 21 54921392.

E-mail addresses: zhaogangtcm@hotmail.com (G. Zhao), lhguo@sibs.ac.cn (L.-H. Guo).

dopamine/c (DA/NE) transporter modulator [15]. Thus, luteolin is a central nervous system (CNS)-oriented compound and has a potential for treating neuropsychological disorders. Moreover, luteolin with active polyphenolic hydroxyl groups is capable of scavenging superoxide radical, hydroxyl radical, 1,1-diphenyl-2-picrylhydrazyl (DPPH) radical and alkyl radical in cultured human endothelial cells [23] and scavenging hydrogen peroxide in OLN-93 oligodendrocytes [24,25], suggesting that luteolin could offer neuroprotective benefit for brain. Accordingly, it is hypothesized that luteolin might act by protection of neuronal cells against free radical injury and thereafter by improvement of the progression of neurodegenerative diseases especially cerebral stroke. In this study, we used an H₂O₂-insulted in vitro platform for screening neuroprotective agents and subsequently an I/R rat model for evaluating their potential anti-ischemia actions. Our primary result showed that luteolin was indeed protective against neuronal injury.

2. Materials and methods

2.1. Preparation of luteolin

2.1.1. Isolation of luteolin

Extraction, purification and structural identification of luteolin (3',4',5,7-tetrahydroxyflavone) from herb material Purple Perilla Fruit were conducted according to the methods reported previously [15]. Its purity was 98%, which was measured by the normalization method following HPLC detection (Beckman Coulter, Fullerton, CA, USA).

2.1.2. Preparation of liposome-encapsulated luteolin (lipLU)

lipLU was adopted for in vivo study. The formulation was prepared by a rotary evaporation technique. Briefly, soy lecithin, cholesterol, vitamin E and luteolin (11.2, 2.8, 0.2, 0.14 and 1.0 g, respectively) were mixed and dissolved in anhydrous ethanol. The solvent was then evaporated (55°C, 0.09 MPa) in a rotary evaporator until a thin layer was formed. The thin layer was then hydrated in an aqueous solution (500 ml) containing poloxamer and sucrose (2.5 and 25 g, respectively) at 50°C. The hydrated mixture was processed by a 30-min ultrasonification to obtain a solvent. After high-pressure homogenization by using a lab-scale homogenizer (EmulsiFlex-B3; Avestin Inc., Ottawa, Canada), lipLU solvent was finally obtained. The mean diameter of the liposomes was around 150 ± 50 nm, which was determined by laser scattering Particle Sizing Systems (PSS Nicomp 380, Santa Barbara, CA, USA), and its encapsulation rate was 98%. The same process was performed on liposomal vehicle, except that no luteolin was added. The lipLU solvent and its vehicle were stored at 4°C for use (usually not more than one week). Such encapsulation was performed for the purpose of enhancing its capability to penetrate the blood–brain barrier (this pharmacokinetic character has been proven in our previous work).

2.2. In vitro screening platform and bioactivity of luteolin

Primary neurons were cultured as described previously [26] with a slight modification. Briefly, cortices of 12-h neonatal Sprague-Dawley (SD) rats were harvested and minced, and then treated with 0.25 mg/ml trypsin and 0.2 mg/ml DNase I. After inactivation of trypsin in Dulbecco's Modified Eagle's (DMEM) medium containing horse serum, the cells were cultured in a B27-supplemented neurobasal culture medium and then done in another medium containing cytarabine (10 μM) for inhibiting nonneuronal cell division. The primary cortical neurons were authenticated by immunofluorescence staining with microtubule-associated protein-2 antibody. Neuroprotectants were screened in vitro by using the neuronal cells exposed to pathogens.

To evaluate the efficacy of luteolin, the primary neurons was treated with vehicle, luteolin, or reference compound (both compounds were dissolved in double distilled water containing 1% dimethylsulfoxide (DMSO) together with 200 μM H₂O₂ and then incubated for 12 h. Cell viability was assayed by 2-(2-methoxy-4-nitrophenyl)-3-(4-nitrophenyl)-5-(2,4-disulphophenyl)-2H-tetrazolium monosodium salt (WST-8) reduction, which was carried out according to the manufacturer instruction manual for cell counting kit-8 (CCK-8) (Dojindo Laboratories, Tokyo, Japan). Activity of WST-8 reduction was represented as OD ratio between the wells containing cells plus compound and the wells containing compound only. By such normalization, the interference by light yellow color of reaction solvent was able to be ruled out.

2.3. In vivo evaluation

2.3.1. Animals

Adult female SD rats (weighing 200–220 g, 2 months of age) were commercially provided from the Laboratory Animal Center of the Chinese Academy of Science (Shanghai, China). Animals were housed at room temperature (22±3°C) under standard 12-h light/dark cycles (lights on at 7 a.m.) with unlimited access to food and water. The rats were acclimated to the room conditions for 1 week prior to experimentation. The experimental protocols were approved by the Laboratory Animal

Center of the Chinese Academy of Science. All procedures involving animals and their care were conducted in compliance with the National Institutes of Health's guidelines regarding the principles of animal care.

2.3.2. Grouping, model establishment and treatment

Rats were randomly separated into four groups: sham group with liposome solvent (*n*=16), model group with liposome solvent (*n*=16), treatment group with 5 mg/kg lipLU (*n*=18), and treatment group with 20 mg/kg lipLU (*n*=18) (we previously showed no difference between control group with normal saline and that with liposome formula in behavioral parameters; thus, no saline group was concluded in this study).

The middle cerebral artery occlusion (MCAO) was performed using the method of Longa et al. [27] with a slight modification. In brief, the rats were anesthetized with chloral hydrate (300 mg/kg ip). The left common carotid artery, external carotid artery (ECA) and internal carotid artery (ICA) were exposed, and the distal end of the ECA was ligated with a 5-0 silk suture. A 5-cm length of nylon filament (diam Ø 0.26 mm; Shandong Bio-Technologies, Beijing, China) with a smooth, soft and flexible tip (which can reduce the risk of vessel injury and intracranial bleeding) was then introduced into ECA through a small puncture and advanced into the middle cerebral artery (MCA) via ICA (18–20 mm, as measured from the carotid bifurcation according to animal weight) until a slight resistance was felt. Such resistance indicated that the filament had passed beyond the proximal segment of the anterior cerebral artery (ACA) (See Fig. 1). At this point, the intraluminal suture blocks the origin of MCA and occluded all sources of blood flow from ICA, ACA and the posterior cerebral artery. Forty minutes after the induction of ischemia, the filament was slowly withdrawn, and the animals were then returned to their cages and given free access to food and water. The same surgical process was performed on sham rats, except that no thread was inserted. As shown in a pretest, 100% of animals were successfully developed into a typical I/P model by experienced technicians of our lab, each with symptom score 3–5, and there was no animal death that occurred during a 2-week experimentation. At 6 h after reperfusion, all grouped animals were subject to a 13-day treatment (once-daily intraperitoneal injection of drug or vehicle). The neurological status of the animals was assessed respectively at 10 h, on Day 7 and on Day 14 after I/R.

2.3.3. Behavioral evaluation

For measuring behavioral deficits, the symptom score was rated as previously reported [28]. All animals were evaluated behaviorally with an operator blinded to groups for spontaneous movement without deficit (Grade 0), forelimb flexion contralateral to injured hemisphere (Grade 1), wire grip deficit with internal rotation (Grade 2), circling to paretic side (Grade 3), circling tightly with head tilt (Grade 4) and spinning or no movement (Grade 5).

Beam-walking test was used for measuring the balancing ability of animals after the symptom score counting [28]. Animals were allowed to walk on a 175-cm-long, 1.9-cm-wide wood beam, and their performance was graded from 6 for a rat that

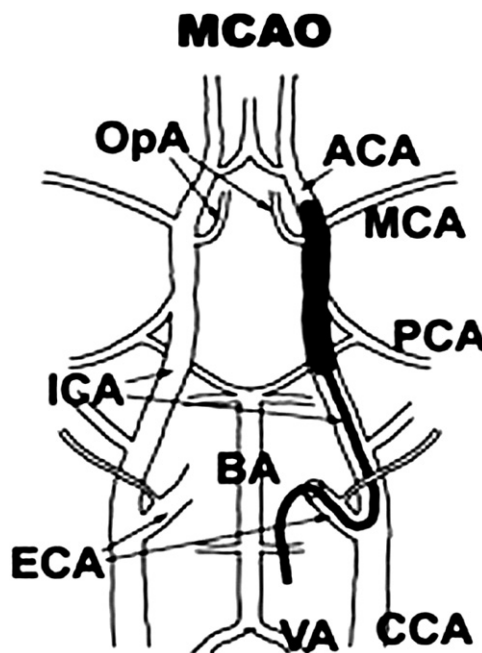


Fig. 1. Schematic drawing of the thread placed into the ECA with its tip proximal to the origin of the MCA. CCA, common carotid artery; PCA, posterior cerebral artery; VA, vertebral artery; BA, basilar artery; OpA, ophthalmic artery.

readily traversed the beam to 0 for a rat that was unable to move or fell off the beam. The seven categories of neurological findings were scored: 0=falling from beam, 1=maintaining body on beam but without moving, 2=falling during crawling, 3=crawling through beam but with hindlimb palsy, 4=crawling through beam but with shuffle step, 5=walking through beam with less shuffle step and 6=walking normally through beam.

2.3.4. 2,3,5-Triphenyltetrazolium chloride (TTC) stain and Cresyl violet-staining

To further assess the neuroprotective effects of luteolin on I/R-induced brain damage, half rats in each group were anesthetized and decapitated after a perfusion of heart with 0.9% normal saline on day 14 after I/R. Their brains were rapidly dissected, frozen, and stored at -20°C for 20 min. The brains were then placed in a rat-brain matrix (SLY-RBM, Beijing Sunny Instruments) and coronally sectioned into 2-mm-thick sections (from 2-mm caudal to the frontal tip). The slices were immediately stained with 2% TTC (Sigma Chemical, St. Louis, MO, USA) solution at 37°C for 30 min in the dark and fixed by immersion in 4% paraformaldehyde in 0.1 M phosphate-buffered saline (PBS). The stained slices were scanned with a high resolution CCD camera (Carl ZEISS, Germany). The total nonischemic or ischemic hemisphere infarct areas were quantified using a CD-8000 Image Analysis System (Britain, UK). The total mean infarct areas of hemisphere (or striatum) were calculated as the average of the area on its rostral and caudal surface. The determined infarct surface areas were added and multiplied by the section thickness (2 mm) to calculate the infarct volume and then recalculated to yield the percentage volume of the contralateral hemisphere.

The TTC-stained slabs were cryoprotected in 25% sucrose in 0.1 M PBS at 4°C for 24 h, then cut with a cryostat (Leica CM 3050 S; Leica, Nussloch, Germany) into $30\text{-}\mu\text{m}$ coronal sections and then processed histologically. Sections were mounted on gelatin-coated microscope slides, allowed to dry at 37°C for 24 h and then stained with cresyl violet for 5 min. Afterwards, they were dehydrated in increasing concentrations of ethanol and finally coverslipped from xylene.

2.3.5. ROS, catalase (CAT) and glutathione (GSH) detection

After behavioral study, the remaining animals were sacrificed and their brains were taken out. Ipsilateral hippocampus, frontal cortex and striatum were dissected and homogenated. Half of the brain homogenate was immersed in an ice-cold isolation buffer (320 mM sucrose, 1 mM EDTA, 0.5 mg/ml BSA, 10 mM Tris-HCl buffer, pH 7.4) and then centrifuged at $2000\times g$ for 2 min, and then the supernatant was centrifuged at $10,000\times g$ for 10 min. The pellet obtained was resuspended in 1 ml of the same isolation buffer and centrifuged at $10,000\times g$ for another 10 min. The pellet obtained was resuspended in 1 ml of incubation buffer (100 mM KCl, 75 mM mannitol, 25 mM sucrose, 0.05 mM EDTA, 0.5 mg/ml BSA, 15 mM Tris-HCl buffer, pH 7.4), and the mitochondria preparation was then obtained, which was used for analyzing ROS content. Mitochondria-generated ROS were determined spectrofluorometrically using the membrane-permeable fluorescent probe 2,7-dichlorodihydrofluorescein diacetate (H_2DCFDA) (Sigma Chemical) [29]. Briefly, mitochondria (40 μg protein) were incubated in a reaction buffer (pH 7.0) containing 250 mM sucrose, 20 mM 3-(N-morpholino) propanesulfonic acid (MOPS), 10 mM Tris, 50 μM EGTA, 0.5 mM Mg^{2+} , 0.1 mM KH_2PO_4 , 1.0 mM cyclosporine A, 10 μM H_2DCFDA , 2.5 mM malate, and 2.5 mM glutamate. After a 40-min incubation at 37°C , the formation of oxidized fluorescent product dichlorofluorescein (DCF) was monitored by an excitation at 488 nm and an emission at 525 nm. The results were expressed as arbitrary fluorescence units per milligram of protein.

The remaining homogenates were treated with cell IP-lysis buffer or detergent M (both from Beyotime Institute of Biotechnology and respectively used for sample preparation in CAT or GSH assay) and centrifuged at $10,000 g$ for 10 min at 4°C to remove debris. The supernatant was used for assaying the activity of CAT or levels of GSH by the methods of He et al. [30] and Bi et al. [31], respectively. Assay kits were purchased from Beyotime Institute of Biotechnology, Shanghai. Protein concentration was measured by the method of Bradford [32] using bovine serum albumin as standard.

2.4. Data analysis

Data were analyzed using SPSS software v.13.0 (Chicago, IL, USA). Values were expressed as mean \pm S.E.M. Analysis of variance (ANOVA) followed by least significant difference (LSD) post hoc tests was used to examine differences between groups. $P < .05$ was considered statistically significant.

3. Results

3.1. In vitro screening of lead compound and validation of its bioactivity

Using the neonatal cortical cell system, we screened neuroprotective agents from a series of CNS-orientated compounds each at concentration of $100\text{ }\mu\text{M}$. Our primary screenings by using lactate dehydrogenase test revealed that luteolin, an isolate of Purple Perilla Fruit, was with a preferential efficacy for lowering the cytotoxicity induced by H_2O_2 (data not shown). Luteolin was therefore adopted as candidate for further study.

For corroborating the initial screen result, luteolin in a broader concentration range, was added to the screen and a sensitive technique WST-8 was used to detect cell viability. As shown in Fig. 2, H_2O_2 ($200\text{ }\mu\text{M}$) administration caused a pronounced inhibitory action on the viability of primary neurons; however, luteolin (at 5, 15, 30 and $90\text{ }\mu\text{M}$) significantly attenuated the cytotoxicity in a concentration-dependent manner; similarly, reference vitamin E (at 15 and $90\text{ }\mu\text{M}$) was also protective against the ROS insult. At concentration of $15\text{ }\mu\text{M}$, the protective action of luteolin was superior to that of vitamin E ($P < .05$), but with both at $90\text{ }\mu\text{M}$, there was no significant difference from each other.

3.2. Effect of lipLU on behavioral deficits

To determine the potential in vivo efficacy of luteolin, a stroke model was established by a 40-min MCAO followed by reperfusion, i.e., I/R model, and then was injected with luteolin in liposome-encapsulated formula at 6 h post-reperfusion daily for 13 successive days. During the whole experimental session, the symptom scores in the model, 5 mg/kg, or 20 mg/kg group seemed to decrease in a time-dependent way, but the score in formula-treated I/R group (model) was largely higher than that in sham group ($P < .01$). Following the first 4-h treatment (treatment beginning at 6 h and measurement at 10 h after I/R), the scores in lipLU-treated I/R groups (luteolin dosage at 5 and 20 mg/kg, respectively) were generally similar to that in the model group. At both Day-7 and Day-14 points, the scores in treatment groups were, however, generally lower than that in respectively day-paired model group, wherein the improving action in the 5 mg/kg group was statistically significant only at day 14 ($P < .05$ vs. model), while that in the 20 mg/kg group was significant not only at Day 7 but also at Day 14 ($P < .01$ for both dose groups vs. respective day-paired model) (Fig. 3).

To further define aspects of neurobehavioral protection, the animals were subjected to another behavioral paradigm, a beam-walking test that is widely used for evaluating limb cooperation and body balance. During the 14-day experimental session, a tendency of time-dependent increase in balance scores was seen in the model, 5 mg/kg or 20 mg/kg group, but the score in the model group was lower than that in sham ($P < .01$) at the three time points. Although the first 4-h treatment with lipLU did not affect the balance deficit in I/R rats, 5 mg/kg-lipLU and 20 mg/kg-lipLU group at Day 7 and Day 14 displayed higher performance scores (on Day 7 or Day 14, $P < .05$ and $.01$, respectively, for the 5 and 20 mg/kg groups vs. respective time point-paired model) (Fig. 4).

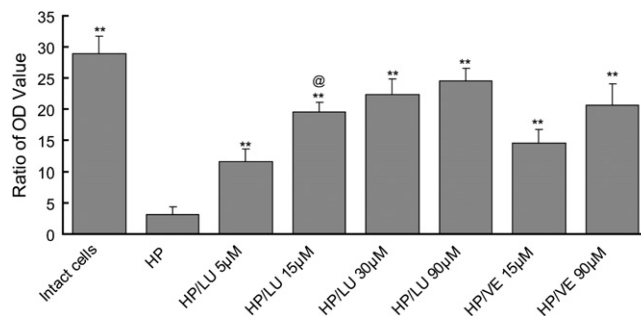


Fig. 2. Neuroprotective actions of luteolin (LU) and vitamin E (VE) on H_2O_2 -insulted neonatal neurons (by CCK-8 test). HP, hydrogen peroxide (H_2O_2). Activity of each cell group was represented as the OD ratio between treatment cell group and concentration-paired, no-cell group. One-way ANOVA, $F_{7,16}=275.45$, $P < .001$. Post-hoc, ** $P < .01$ vs. HP-only; @ $P < .05$ vs. HP plus VE $15\text{ }\mu\text{M}$. Values are expressed as mean \pm S.E.M. of triplicate cell samples.

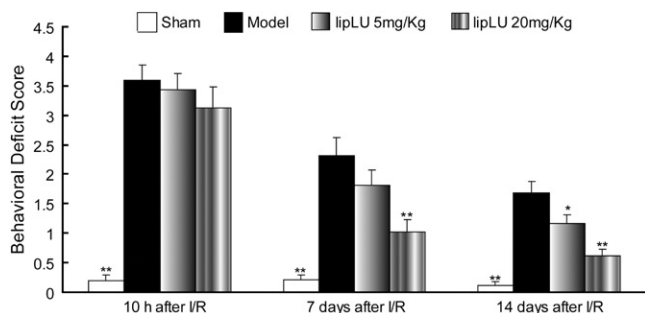


Fig. 3. Effect of luteolin on symptom score of I/R rats. Symptom score of each animal was rated at 10 h (4 h after treatment onset), on Day 7 and on Day 14 after reperfusion. At each time point, $F_{3,64}=28.45$, 55.3 and 147.36 , respectively for the time points of 10 h, Day 7 and Day 14, all $P<.01$ (by one-way ANOVA, same as mentioned below). Post hoc, $*P<.05$ and $**P<.01$ and, respectively, vs. corresponding day-paired model group (by LSD, same as mentioned below). Data were expressed as mean \pm S.E.M. of 16–18 animals.

3.3. Effect of lipLU on histological lesion

TTC is converted to red formazone pigment by nicotinamide adenine dinucleotide (NAD) and dehydrogenase present in living cells. Hence, viable cells were stained deep red. The infarcted cells have lost the enzyme and, thus, remained unstained dull yellow as observed in the model group. Unlike the control group that showed a less red staining, groups with luteolin in liposome formula showed an increased red staining (Fig. 5A) after successful 13 daily administrations. The electronic pictures of cerebral slices were processed by software, and then the mean infarction volume was obtained. Volume in the model group is $38.2 \pm 9.2\%$ or $54.1 \pm 14.1\%$ of contralateral hemisphere, respectively, for striatum or hemisphere. The brain slices of two treatment groups showed lower levels of infarction volume in the region of hemisphere (or striatum) than that of model group ($P<.05$ and 0.01 , respectively, for the 5 and 20 mg/kg groups) (Fig. 5B).

Another morphological evaluation was conducted by using the method of cresyl violet stain (Nissl staining). As shown in Fig. 6A, sections in the model group showed a sparser cresyl violet staining in CA1 and CA2 subregions of hippocampus (especially to pyramidal neurons) than that in sham, while sections of 5 and 20 mg/kg groups exhibited a denser staining in both subregions relative to model. As shown in Fig. 6B, the neuronal cell shape in CA1 in the model group was prominently changed from a big round in normal group to a small multi-shape pattern, i.e., irregular, moon, or triangle shape with an uneven color, and most of cells were shrunken with some loss of

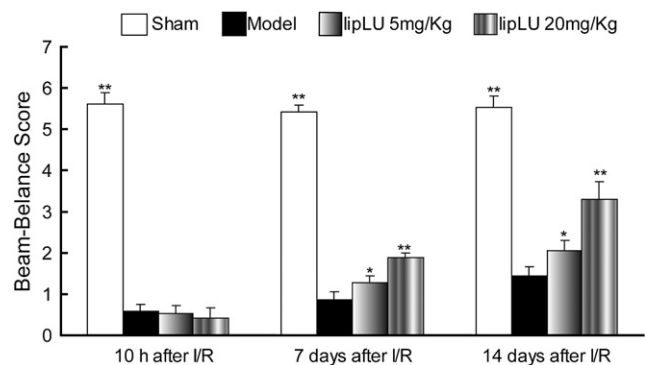


Fig. 4. Effect of luteolin on the balance performance of I/R rats. Balance behavior of each animal was evaluated at 10 h, on Day 7 and on Day 14 after reperfusion. At each time point, $F_{3,64}=47.11$, 103.51 and 237.06 , respectively, for the 1, 7 and 14-day time point, all $P<.01$. Post hoc, $*P<.05$ and $**P<.01$, respectively, vs. same-day-paired model group. Data were expressed as mean \pm S.E.M. of 16–18 animals.

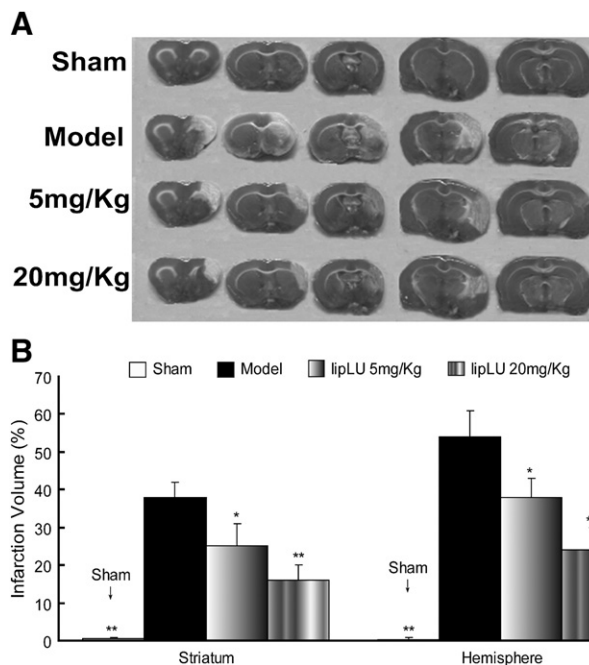


Fig. 5. Effect of luteolin on TTC stain (A) and the infarction volume (B) of I/R rats. TTC staining was performed after the final behavioral test, and infarction volume of each slab was calculated. Data were expressed as percent of volume of contralateral hemisphere (mean \pm S.E.M. of 8–9 animals). $F_{3,30}=43.75$ and $F_{3,30}=59.16$, respectively, for hemisphere and striatum, both $P<.01$. Post hoc, $*P<.05$ and $**P<.01$, respectively, vs. respective model group.

nucleus and/or cytoplasm accompanied by glial hyperplasia. However, lipLU treatment conferred a relatively pronounced protection against the abnormality of cell shape and size, and the most striking effect was shown in the group with 20 mg/kg of lipLU, in which the neurons in CA1 were relatively round and intact with relatively clear nucleus and/or cytoplasm, generally resembling those observed in the animals of sham group. Besides, the phenomenon of glial hyperplasia was not seen in the group of 20 mg/kg lipLU. Similar changes of cell shape in the model group and neuroprotection by luteolin in treatment groups were also seen in the ischemic penumbral region of the parietal cortex (Fig. 6C).

3.4. Effects of luteolin on mitochondrial ROS generation in I/R rats' brain

Mitochondria-generated ROS was measured by incubation of sample with fluorescent probe 2',7'-dichlorodihydrofluorescein. As shown in Fig. 7, the DCF-fluorescence was substantially increased in ipsilateral hippocampi, frontal cortices and striata harvested from brains of model rats (that had already gone through a 14-day I/R threat) (in all the three brain regions, $P<.05$ or $.01$ vs. sham rats). However, the increased ROS was significantly inhibited following a 13-day luteolin treatment (both luteolin dosages toward the three regions, all $P<.05$ or $.01$ vs. model, with exception of 5 mg/kg statistically significant only in frontal cortex).

3.5. Effects of luteolin on catalase and glutathione in I/R rats' brain

Detections of catalase and glutathione was performed on day 14 after reperfusion. As shown in Fig. 8, the CAT and GSH levels in ipsilateral hippocampi, frontal cortices, and striata harvested from brains of model group were significantly lower than that of sham rats. However, luteolin treatment reversed the decreases of CAT and GSH levels in the three brain regions of I/R rats, wherein for CAT (Fig. 8A), the 5 mg/kg dosage group showed a statistically significant action in

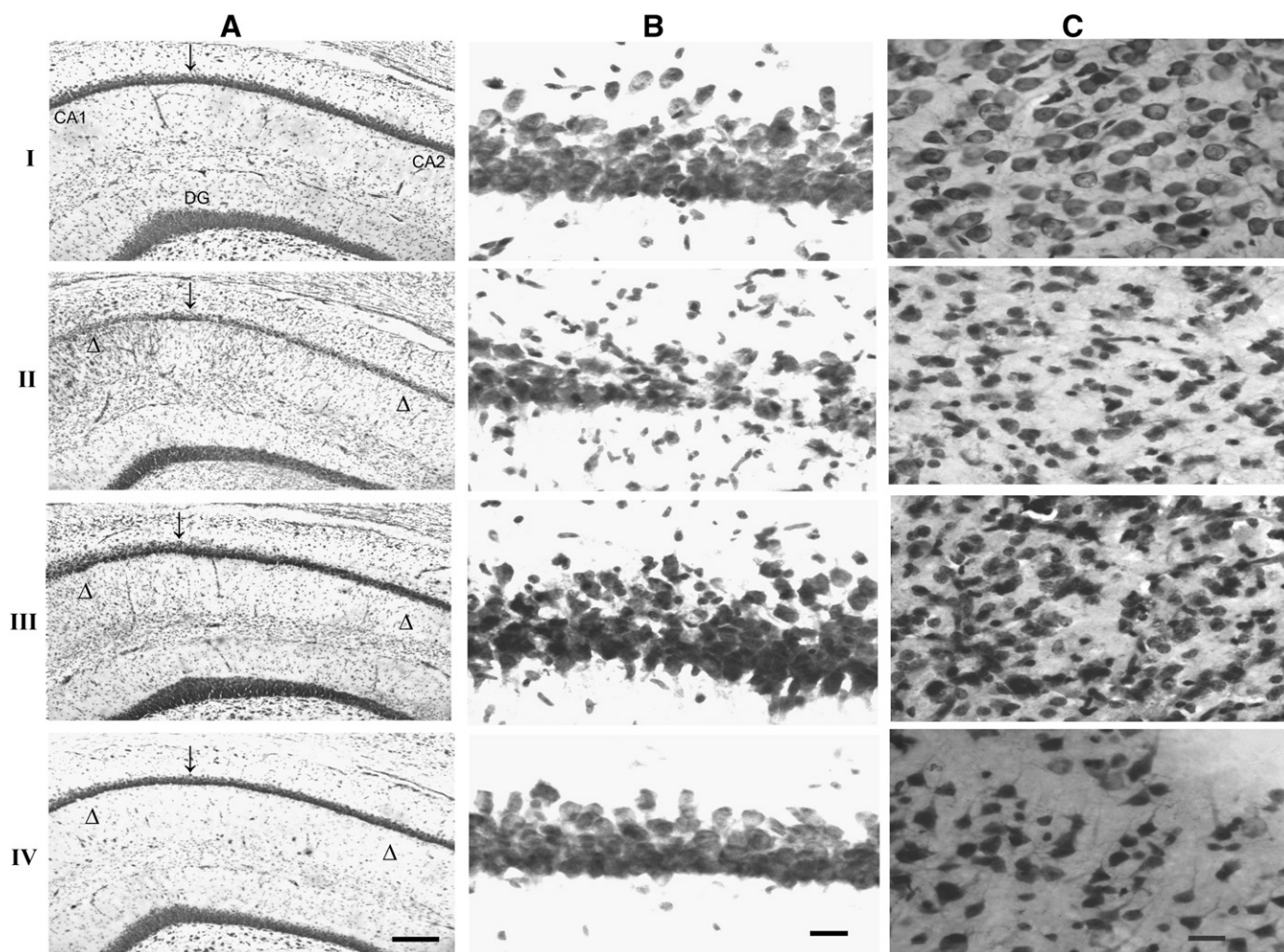


Fig. 6. Protective action of luteolin on neuronal cells in hippocampus and ischemic penumbra in I/R rats (assayed by cresyl violet staining). (A) Sections of hippocampus with scale bar of 200 μm ; arrows, indicating the regions enlarged for Fig. 6B. (B) Sections of hippocampus with scale bar=20 μm . (C) Cell shape in ischemic penumbral region of parietal cortex (scale bar=20 μm); parietal cortex in sham, serving as control. Panels I, II, III and IV in column A, B or C, representing sham, model, LipLU 5 mg/kg, and LipLU 20 mg/kg group, respectively. DG, dentate gyrus; Δ , injured regions.

frontal cortex ($P<.05$ vs. model), while the 20 mg/kg group showed significance in the three brain regions ($P<.05$ or .01, respectively, vs. model); for GSH (Fig. 8B), 5 mg/kg dosage group showed a statistically significant action in frontal cortex and striatum ($P<.05$, respectively, vs. model), while 20 mg/kg dosage was significant in the three brain regions ($P<.01$, respectively, vs. model).

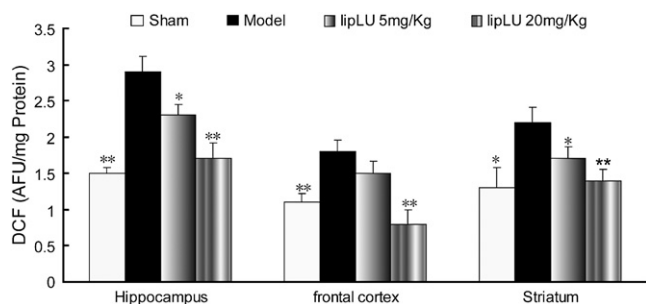


Fig. 7. Effect of luteolin on the level of ROS (DCF) in I/R rats' brain. DCF levels were assayed upon the mitochondria prepared from the ipsilateral hippocampus, frontal cortex and striatum of rats. $*P<.05$ and $**P<.01$, respectively, vs. respective model group. Data were expressed as mean \pm S.E.M. of eight to nine animals.

4. Discussion

Free radicals have been the focus of interest as candidates for elucidation of ischemia responses and potential therapeutic agents. ROS threaten neuronal survival by their ability to propagate the initial attack on protein/lipid-rich membranes to cause lipid peroxidation [33], protein glycation, enzyme inactivation and then alteration in the structure and function of neuronal cells [34]. Accordingly, our drug-screening model established by administration of exogenous ROS (H_2O_2) to primary neurons may primarily reproduce the major pathological change of neurodegenerative disorders and was able to serve as a suitable platform for primarily screening clinically meaningful neuroprotectants. Upon the platform, phytochemical luteolin markedly reversed the cytotoxicity induced by H_2O_2 , an action that is likely due to an antioxidant mechanism because such effectiveness is somewhat similar to that of potent antioxidant vitamin E (Fig. 2). Thus, luteolin would be effective for treatment of ischemia stroke in animals.

To testify this supposition, an in vivo model of cerebral ischemia needs to be established. Previously, the pathological changes in patients were successfully modeled by using the method of silicon-coated thread embolization in cerebral arteries of rats. The related models have been widely used for assessing the pathophysiological

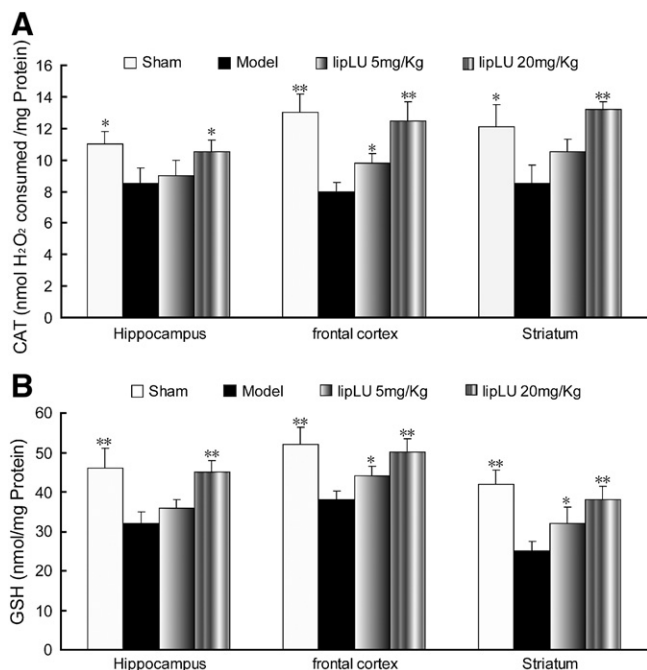


Fig. 8. Effect of luteolin on the level of CAT and reduced GSH of I/R rat brain. Levels of CAT (A) and GSH (B) in ipsilateral hippocampus, frontal cortex and striatum were assayed by using the CAT and GSH kits. * $P < .05$ and ** $P < .01$, respectively, vs. respective model group. Data were expressed as mean \pm S.E.M. of eight to nine animals.

and therapeutic implications in ischemia stroke [28]. MCAO model is capable of mimicking many features of the stroke in humans, since MCA, as a specific occlusion site in this model, is the most commonly blocked vessel in patients of thrombotic strokes [28,35]. Following cerebral artery occlusion, reperfusion is also a naturally occurring clinical event [36]. Thus, reperfusion after MCAO in animals confers characteristics more similar to ischemia stroke in human than a sole MCAO. In this study, I/R model was adopted for evaluating the possible *in vivo* neuroprotective effect of luteolin. Rats in control groups expressed a severe abnormality of behavior such as limb palsy and body imbalance during a 2-week observation (Fig. 3, Fig. 4), demonstrating that I/R model was established successfully. However, this model is characterized by a little restoration of behavioral abnormality within the 14-day session, indicating a possible post-stroke neurogenesis in the brains of this model. This phenomenon is consistent with the finding reported previously [37]. The *in vivo* model is also validated by the evidence of histological lesion as observed in TTC (Fig. 5) and cresyl violet stain on the final day (Fig. 6).

Several plant-derived polyphenols offered neuroprotections against the pathological process of ischemia [38]. Using the I/R model, we assessed the potential anti-ischemic action of lipLU. Although many approaches including free radical scavengers and anti-apoptotic and anti-inflammatory agents were tried [35] for abating acute ischemic change or I/R damage, pre-ischemic dosage of animals is a common schedule adopted by majority of researchers and up to now, few preclinical studies have demonstrated an anti-ischemic efficacy by using a post-ischemic paradigm similarly to clinical therapy. For accurately evaluating the potential clinical meaningfulness, the therapeutic window (TW) for lipLU administration was defined at 6 h following I/R on the basis of the optimal TW that is commonly adopted clinically during thrombolytic treatment and also according to the reports that viable TW for several neuroprotective agents was proposed to extend to as late as 4–6 h after vessel blockade or I/R [39,40]. Our current study showed that multiple administration of lipLU to the I/R model beginning at 6 h

post-reperfusion elicited a profound decrease of symptom score and a pronounced enhancement of balance score on Day 7, and the behavioral improvements were even more obvious on Day 14 after reperfusion (Fig. 3, Fig. 4), demonstrating a delayed effect in protection of I/R rats against the deficiency of behavioral performance. Such behavior-improving actions indicated that lipLU possessed a long-lasting anti-ischemic activity, which was confirmed by subsequent histological detections on brain slices that showed a delayed action in improvement of the histological injury after lipLU treatment (Fig. 5, Fig. 6). The ability to ameliorate the behavioral and morphological changes demonstrates that luteolin given postischemically conferred a delayed neuroprotective action that may be clinically meaningful. This liposome-encapsulated luteolin (itself or as an adjunct to thrombolytic therapy) could serve as a long-acting medication regimen for treating progressive cerebral ischemia. Also, results from this study will pave the way for future investigations of not only the protective effects of luteolin but also the possible protective actions of other polyphenolic compounds against post-stroke damage.

Under physiological condition, the regulation of free radicals is controlled by endogenous antioxidant defense system that removes excessive free radicals. Oxidative stress states a disturbance of pro-oxidant–antioxidant homeostasis, namely, an oxidant/antioxidant imbalance that has been clearly shown to be involved in the pathogenesis of neurodegenerative diseases by several studies [41]. Our study showed that I/R resulted in not only an increase of ROS production (Fig. 7) but also an inhibition of endogenous antioxidant defense system (CAT and GSH, as major markers of antioxidant system) in rat brains (Fig. 8), indicative of an occurrence of imbalance between the oxidant and antioxidant networks, which is known to be involved in varieties of proapoptotic cascades [42] and has recently become the subject of intense study in the field of neurodegenerative disorders [43]. It is important to mention that luteolin toward I/R rats conferred reversing actions on the increase of ROS production (Fig. 7) and, simultaneously, on the decreases of endogenous antioxidant GSH and CAT activity (Fig. 8), indicating that luteolin improves the I/R-induced brain damage likely by delicately rebalancing the aberrated pro-oxidant/antioxidant force. Novel cytoprotective strategies responding to imbalance in the oxidant/antioxidant status may effectively delay neurodegenerative process in human [43,44].

To date, several potent antioxidants have been uncovered, e.g., pure scavenger molecules such as boldine [45], N-methyl-D-aspartic acid (NMDA) receptor blockers [46] and chain-breaking vitamin E [47], most of which, however, act via an one-target mechanism and fail clinically to protect neurons from free radical damage. Cerebral I/R trigger a series of pathophysiological and biochemical changes in the brain that present multiple targets for therapeutic intervention [48]. Although free radicals have long been thought to be major contributors for brain damage following stroke or I/R [49], inflammatory factors are also considered to play roles in the pathogenesis and treatment of cerebral ischemia [50]. Besides its balancing mechanism for the aberrated oxidant/antioxidant status, as demonstrated in this study, luteolin is also known to have anti-inflammatory [51,52], immunomodulating [53], phytoestrogen-like [54], matrix metalloproteinases-inhibitory [55,56], eNOS (endothelial nitric oxide)-enhancing [57], calcium channel/calpain-inhibitory [58,60], antithrombotic (anti-platelet) [59] and anxiolytic-like [20] activities as well as blockade of mitochondrial cytochrome c release [60] in differing disease models of *in vitro* and *in vivo*, though these actions have not yet been explored on stroke models with luteolin. Moreover, luteolin is able to activate nuclear factor erythroid-2-related factor 2, a transcription factor central to the enhancement of cerebral oxidative stress defense, maintenance of the cellular redox homeostasis and intervention of neurodegenerative diseases, in an ERK-dependent way in PC12 and C6 cells insulted with N-methyl-4-

phenyl-pyridinium [61]. In fact, any casual pathway responsible for the aforementioned actions is also thought to participate, albeit to different extents, in the progression of cerebral ischemia, and modulation of respective pathway in turn implicates somewhat an intervention for this disease. This unique advantage in target attribution elicits a hypothesis that the delayed neuroprotection of luteolin in the I/R model might be due to a synergistic regulation at multitargeting sites.

In summary, plant-derived luteolin acts by neuroprotection in primary cultured neurons exposed to oxidative stress and anti-ischemia in animals insulted by I/R, possibly by correction of oxidant/antioxidant imbalance. Luteolin itself is actually a naturally occurring compound found in a wide variety of dietary plants. With the possible property of synergistic effects at multiple target sites, the food-derived luteolin in liposomal formula may serve as a neuroprotective dietary supplement or pharmaceutical, which would provide a considerable health benefit either for subject at risk or in therapy following episodes of ischemic stroke. The multitarget mechanisms for the delayed neuroprotection by postischemic treatment with luteolin will be further explored in near-future study.

Acknowledgments

We thank Mr. Jie Wang for help in cell culture and Mr. Kai Wang in histological manipulation. We also thank Mr. Long-Fei Xu, Ms. Jun Zhao and Ms. Ying Li for skillful technical assistance in establishment of in vivo model and behavioral detection. All the authors and persons in the acknowledgments are employees of Cell Star Bio-Technologies and/or Shanghai Institutes for Biological Sciences and Chinese Academy of Sciences and have no conflict of interest. This research was supported by a grant from the Shanghai government (05DZ19339) and Chinese Academy of Science.

References

- [1] Johnston KC, Li JY, Lyden PD, Hanson SK, Feasby TE, Adams RJ, et al. Medical and neurological complications of ischemic stroke: experience from the RANTAS trial. RANTAS Investigators. Stroke 1998;29:447–53.
- [2] Hicks A, Jolkkonen J. Challenges and possibilities of intravascular cell therapy in stroke. Acta Neurobiol Exp 2009;69:1–11.
- [3] Shin WH, Park SJ, Kim EJ. Protective effect of anthocyanins in middle cerebral artery occlusion and reperfusion model of cerebral ischemia in rats. Life Sci 2006;79:130–7.
- [4] Mehta SL, Manhas N, Raghuraj R. Molecular targets in cerebral ischemia for developing novel therapeutics. Brain Res Rev 2007;54:34–66.
- [5] Neumar RW. Molecular mechanisms of ischemic neuronal injury. Ann Emerg Med 2000;6:483–506.
- [6] Collino M, Aragno M, Mastrocola R, Gallicchio M, Rosa AC, Dianzani C, et al. Modulation of the oxidative stress and inflammatory response by PPAR-gamma agonists in the hippocampus of rats exposed to cerebral ischemia/reperfusion. Eur J Pharmacol 2006;530:70–80.
- [7] Barinaga M. Stroke damaged neurons may commit cellular suicide. Science 1998;281:1302–3.
- [8] Kelly PJ, Morrow JD, Ning M, Koroshetz W, Lo EH, Terry E, et al. Oxidative stress and matrix metalloproteinase-9 in acute ischemic stroke: the Biomarker Evaluation for Antioxidant Therapies in Stroke (BEAT-Stroke) study. Stroke 2008;39:100–4.
- [9] Jia J, Guan D, Zhu W, Alkayed NJ, Wang MM, Hua Z, et al. Estrogen inhibits Fas-mediated apoptosis in experimental stroke. Exp Neurol 2009;215:48–52.
- [10] Donnini S, Solito R, Monti M, Balduini W, Carloni S, Cimino M, et al. Prevention of ischemic brain injury by treatment with the membrane penetrating apoptosis inhibitor, TAT-BH4. Cell Cycle 2009;8:1271–8.
- [11] Love S. Apoptosis and brain ischaemia. Prog Neuropsychopharmacol Biol Psychiatr 2003;27:267–82.
- [12] Zhang HY, Yang DP, Tang GY. Multipotent antioxidants: from screening to design. Drug Discov Today 2006;11:749–54.
- [13] Korotkikh I, Senikienė Z, Simonienė G, Lazauska R, Laukevičienė A, Kevelaitis E. Inotropic and lusitropic effects of *Perilla frutescens* (L.) Britton extract on the rabbit myocardium. Medicina (Kaunas) 2006;42:406–12.
- [14] Meng L, Lozano YF, Gaydou EM, Li B. Antioxidant activities of polyphenols extracted from *Perilla frutescens* varieties. Molecules 2008;14:133–40.
- [15] Zhao G, Qin GW, Wang J, Chu WJ, Guo LH. Functional activation of monoamine transporters by luteolin and apigenin isolated from the fruit of *Perilla frutescens* (L.) Britt. Neurochem Int 2010;56:168–76.
- [16] Van Zanden JJ, Geraets L, Wortelboer HM, van Bladeren PJ, Rietjens IM, Cnubben NH. Structural requirements for the flavonoid-mediated modulation of glutathione S-transferase P1-1 and GS-X pump activity in MCF7 breast cancer cells. Biochem Pharmacol 2004;67:1607–17.
- [17] Verbeek R, van Tol EA, van Noort JM. Oral flavonoids delay recovery from experimental autoimmune encephalomyelitis in SJL mice. Biochem Pharmacol 2005;70:220–8.
- [18] Hou Y, Wu J, Huang Q, Guo L. Luteolin inhibits proliferation and affects the function of stimulated rat synovial fibroblasts. Cell Biol Int 2009;33:135–47.
- [19] Kumazawa Y, Kawaguchi K, Takimoto H. Immunomodulating effects of flavonoids on acute and chronic inflammatory responses caused by tumor necrosis factor alpha. Curr Pharm Des 2006;12:4271–9.
- [20] Coleta M, Campos MG, Cotrim MD, Lima TC, Cunha AP. Assessment of luteolin (3',4',5,7-tetrahydroxyflavone) neuropharmacological activity. Behav Brain Res 2008;189:75–82.
- [21] Tsai FS, Peng WH, Wang WH, Wu CR, Hsieh CC, Lin YT, et al. Effects of luteolin on learning acquisition in rats: involvement of the central cholinergic system. Life Sci 2007;80:1692–8.
- [22] Choi SH, Hur JM, Yang EJ, Jun M, Park HJ, Lee KB, et al. Beta-secretase (BACE1) inhibitors from *Perilla frutescens* var. *acuta*. Arch Pharm Res 2008;31:183–7.
- [23] Choi JS, Choi YJ, Park SH, Kang JS, Kang YH. Flavones mitigate tumor necrosis factor-alpha-induced adhesion molecule upregulation in cultured human endothelial cells: role of nuclear factor-kB. J Nutr 2004;134:1013–9.
- [24] van Meeteren ME, Hendriks JJ, Dijkstra CD, van Tol EA. Dietary compounds prevent oxidative damage and nitric oxide production by cells involved in demyelinating disease. Biochem Pharmacol 2004;67:967–75.
- [25] Afanas' av IB, Dorozhko AI, Brodskii AV, Kostyuk VA, Potapovich AI. Chelating and free radical scavenging mechanisms of inhibitory action of rutin and quercetin in lipid peroxidation. Biochem Pharmacol 1989;38:1763–9.
- [26] Singer CA, Figueroa-Masot XA, Batchelor RH, Dorsa DM. The mitogen-activated protein kinase pathway mediates estrogen neuroprotection after glutamate toxicity in primary cortical neurons. J Neurosci 1999;19:2455–63.
- [27] Salim S, Ahmad M, Zafar KS, Ahmad AS, Islam F. Protective effect of *Nardostachys jatamansi* in rat cerebral ischemia. Pharmacol Biochem Behav 2003;74:481–6.
- [28] Hunter AJ, Hatcher J, Virley D, Nelson P, Irving E, Hadingham SJ, et al. Functional assessments in mice and rats after focal stroke. Neuropharmacology 2000;39:806–16.
- [29] Maciel EN, Vercesi AE, Castilho RF. Oxidative stress in Ca²⁺-induced membrane permeability transition in brain mitochondria. J Neurochem 2001;79:1237–45.
- [30] He Z, Sun X, Mei G, Yu S, Li N. Nonclassical secretion of human catalase on the surface of CHO cells is more efficient than classical secretion. Cell Biol Int 2008;32:367–73.
- [31] Bi J, Jiang B, Liu JH, Zhang XL, An LJ. Protective effects of catalpol against H₂O₂-induced oxidative stress in astrocytes primary cultures. Neurosci Lett 2008;442:224–7.
- [32] Bradford MM. A rapid and sensitive method for the quantification of microgram quantities of protein utilizing the principle of protein-dye binding. Anal Biochem 1976;72:248–54.
- [33] Kale M, Rathore N, John S, Bhatnagar D. Lipid peroxidative damage on pyrethroid exposure and alterations in antioxidant status in rat erythrocytes: a possible involvement of reactive oxygen species. Toxicol Lett 1999;105:197–205.
- [34] Deguchi K, Hayashi T, Nagotan S, Sehara Y, Zhang H, Tsuchiya A, et al. Reduction of cerebral infarction in rats by biliverdin associated with amelioration of oxidative stress. Brain Res 2008;1188:1–8.
- [35] Yousuf S, Atif F, Ahmad M, Hoda N, Ishrat T, Khan B, et al. Resveratrol exerts its neuroprotective effect by modulating mitochondrial dysfunctions and associated cell death during cerebral ischemia. Brain Res 2009;1250:242–53.
- [36] Molina CA, Alvarez-Sabín J, Montaner J, Abilleira S, Arenillas JF, Coscojuela P, et al. Thrombolysis-related hemorrhagic infarction: a marker of early reperfusion, reduced infarct size, and improved outcome in patients with proximal middle cerebral artery occlusion. Stroke 2002;33:1551–6.
- [37] Kidd PM. Integrated brain restoration after ischemic stroke – medical management, risk factors, nutrients, and other interventions for managing inflammation and enhancing brain plasticity. Altern Med Rev 2009;14:14–35.
- [38] Simonyi A, Wang Q, Miller RL, Yusuf M, Shelat PB, Sun AY, et al. Polyphenols in cerebral ischemia: novel targets for neuroprotection. Mol Neurobiol 2005;31:135–47.
- [39] Schneider A, Wysocki R, Pitzer C, Krüger C, Laage R, Schwab S, et al. An extended window of opportunity for G-CSF treatment in cerebral ischemia. BMC Biol 2006;4:36.
- [40] Simard JM, Yurovsky V, Tsymalyuk N, Melnichenko L, Ivanova S, Gerzanich V. Protective effect of delayed treatment with low-dose glibenclamide in three models of ischemic stroke. Stroke 2009;40:604–9.
- [41] Loh KP, Huang SH, De Silva R, Tan BK, Zhu YZ. Oxidative stress: apoptosis in neuronal injury. Curr Alzheimer Res 2006;3:327–37.
- [42] Simon HU, Haj-Yehia A, Levi-Schaffer F. Role of reactive oxygen species (ROS) in apoptosis induction. Apoptosis 2000;5:415–8.
- [43] Calabrese V, Colombrita C, Sultana R, Scapagnini G, Calvani M, Butterfield DA, et al. Redox modulation of heat shock protein expression by acetylcarnitine in aging brain: relationship to antioxidant status and mitochondrial function. Antioxid Redox Signal 2006;8:404–16.
- [44] Calabrese V, Bates TE, Stella AM. NO synthase and NO-dependent signal pathways in brain aging and neurodegenerative disorders: the role of oxidant/antioxidant balance. Neurochem Res 2000;25:1315–41.

- [45] Schmeda-Hirschmann G, Rodriguez JA, Theoduloz C, Astudillo SL, Feresin GE, Tapia A. Free-radical scavengers and antioxidants from *Peumus boldus* Mol. ("Boldo"). *Free Radic Res* 2003;37:447–52.
- [46] Vural M, Arslantaş A, Yazihan N, Köken T, Uzuner K, Arslantaş D, et al. NMDA receptor blockage with 2-amino-5-phosphonovaleric acid improves oxidative stress after spinal cord trauma in rats. *Spinal Cord* 2009;100, doi:10.1038/sc.
- [47] Hensley K, Benaksas EJ, Bolli R, Comp P, Grammas P, Hamdheydari L, et al. New perspectives on vitamin E: gamma-tocopherol and carboxylthylhydroxychroman metabolites in biology and medicine. *Free Radic Biol Med* 2004;36: 1–15.
- [48] Chen SD, Lee JM, Yang DI, Nassief A, Hsu CY. Combination therapy for ischemic stroke: potential of neuroprotectants plus thrombolytics. *Am J Cardiovasc Drugs* 2002;2:303–13.
- [49] Urabe T, Yamasaki Y, Hattori N, Yoshikawa M, Uchida K, Mizuno Y. Accumulation of 4-hydroxynonenal-modified proteins in hippocampal CA1 pyramidal neurons precedes delayed neuronal damage in the gerbil brain. *Neuroscience* 2000;100: 241–50.
- [50] Spagnoli LG, Mauriello A, Sangiorgi G, Fratoni S, Bonanno E, Schwartz RS, et al. Extracranial thrombotically active carotid plaque as a risk factor for ischemic stroke. *JAMA* 2004;292:1845–52.
- [51] Chen CY, Peng WH, Tsai KD, Hsu SL. Luteolin suppresses inflammation-associated gene expression by blocking NF-kappaB and AP-1 activation pathway in mouse alveolar macrophages. *Life Sci* 2007;81:1602–14.
- [52] Kris-Etherton PM, Lefevre M, Beecher GR, Gross MD, Keen CL, Etherton TD. Bioactive compounds in nutrition and health research methodologies for establishing biological function: the antioxidant and anti-inflammatory effects of flavonoids on atherosclerosis. *Annu Rev Nutr* 2004;24:511–38.
- [53] Theoharides TC. Luteolin as a therapeutic option for multiple sclerosis. *J Neuroinflammation* 2009;6:29.
- [54] Liu R, Gao M, Qiang GF, Zhang TT, Lan X, Ying J, et al. The anti-amnesic effects of luteolin against amyloid β_{25-35} peptide-induced toxicity in mice involve the protection of neurovascular unit. *Neuroscience* 2009;162:1232–43.
- [55] Bellosta S, Bogani P, Canavesi M, Galli C, Visioli F. Mediterranean diet and cardioprotection: wild artichoke inhibits metalloproteinase 9. *Mol Nutr Food Res* 2008;52:1147–52.
- [56] Lee H, Stevenson E, Lederer M, Furie KL. Oxidative stress and matrix metalloproteinase-9 in acute ischemic stroke: the Biomarker Evaluation for Antioxidant Therapies in Stroke (BEAT-Stroke) study. *Stroke* 2008;39:100–4.
- [57] Li H, Xia N, Brausch I, Yao Y, Förstermann U. Flavonoids from artichoke (*Cynara scolymus* L.) up-regulate endothelial-type nitric-oxide synthase gene expression in human endothelial cells. *J Pharmacol Exp Ther* 2004;310:926–32.
- [58] Guerrero JA, Navarro-Nuñez L, Lozano ML, Martínez C, Vicente V, Gibbins JM, et al. Flavonoids inhibit the platelet TxA(2) signalling pathway and antagonize TxA(2) receptors (TP) in platelets and smooth muscle cells. *Br J Clin Pharmacol* 2007;64: 133–44.
- [59] Middleton Jr E, Kandaswami C, Theoharides TC. The effects of plant flavonoids on mammalian cells: implications for inflammation, heart disease, and cancer. *Pharmacol Rev* 2000;52:673–751.
- [60] Song J, Liu K, Yi J, Zhu D, Liu G, Liu B. Luteolin inhibits lysophosphatidylcholine-induced apoptosis in endothelial cells by a calcium/mitochondrion/caspases-dependent pathway. *Planta Med* 2010;76:433–8.
- [61] Wruck CJ, Claussen M, Fuhrmann G, Römer L, Schulz A, Pufe T, et al. Luteolin protects rat PC12 and C6 cells against MPP+ induced toxicity via an ERK dependent Keap1-Nrf2-ARE pathway. *J Neural Transm Suppl* 2007;72:57–67.